Characterization of Chemical Reactions Coupled to Electron Transfer Reactions Using Cyclic Voltammetry

Adrian W. Bott, Ph.D.

Bioanalytical Systems, Inc.
2701 Kent Avenue
West Lafayette, IN
47906-1382

awb@bioanalytical.com

Digital simulation is used to illustrate some of the characteristic cyclic voltammograms for selected electrochemical mechanisms in which the electron transfer reactions are coupled to chemical reactions.

Cyclic voltammetry (CV) is widely used for the initial characterization of electrochemically active systems. In addition to indicating the number of different oxidation states, and their relative energies, CV can also be used for mechanistic studies of systems in which the electron transfer reactions are coupled to chemical reactions, due to the characteristic appearance of cyclic voltammograms associated with different mechanisms (1). These characteristically shaped voltammograms are the subject of this article.

The cyclic voltammogram for a reversible process (i.e., the surface concentrations of the oxidized and reduced species required by the Nernst equation are maintained at all potentials) is shown in **F1** for the reaction $O + e = R$. The separation of the peak potentials on the forward (reduction) and reverse (oxidation) scans (ΔE_p) is about 58 mV (at 25 °C) (2), and the magnitudes of the two peak currents are equal (the peak current ratio, i_{pa}/i_{pc}, = 1). The coupling of chemical reactions to the

electron transfer reactions can lead to changes in the peak potentials and/or the peak currents, and the effect of chemical reactions is often expressed in terms of changes in the peak current ratio and/or peak potentials. In addition, in this article, the effects of chemical reactions are also shown using cyclic voltammograms generated by DigiSim®, a simulation program for CV.

When considering the effect of chemical reactions, it is very important to note that any variations from reversible behavior are related not to the absolute magnitude of the rate constant for the chemical reaction (k), but to the value of this rate constant relative to the time scale of the experiment. For example, decreasing the time scale of the experiment also decreases the time available for the chemical reaction, and hence the effect of the chemical reaction can be decreased. The time scale of a cyclic voltammetry experiment is determined by the scan rate ν (increasing the scan rate decreases the experimental time scale); therefore, the im-

portant parameter in determining the effect of chemical reactions is k/ν. In the following examples, simulated voltammograms are shown for different mechanisms at different values of k/ν (where k is the rate of the forward chemical reaction), unless specified otherwise (3).

The nomenclature used to describe the mechanisms is based on E for an electron transfer reaction and C for a chemical reaction; for example, an EC mechanism consists of an electron transfer reaction (E) followed by a chemical reaction (C). Unless stated otherwise, the following parameter values were used for all simulations: $E^o = 0$ V, scan rate = 1 V s^{-1}, $k_s = 1$ cm s^{-1}, $\alpha = 0.5$. These values were selected so that there would be no interfering effects from slow heterogeneous electron transfer kinetics.
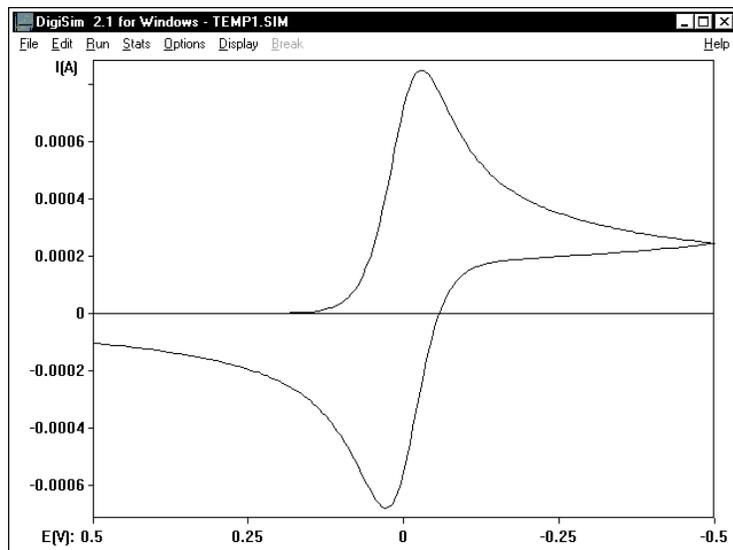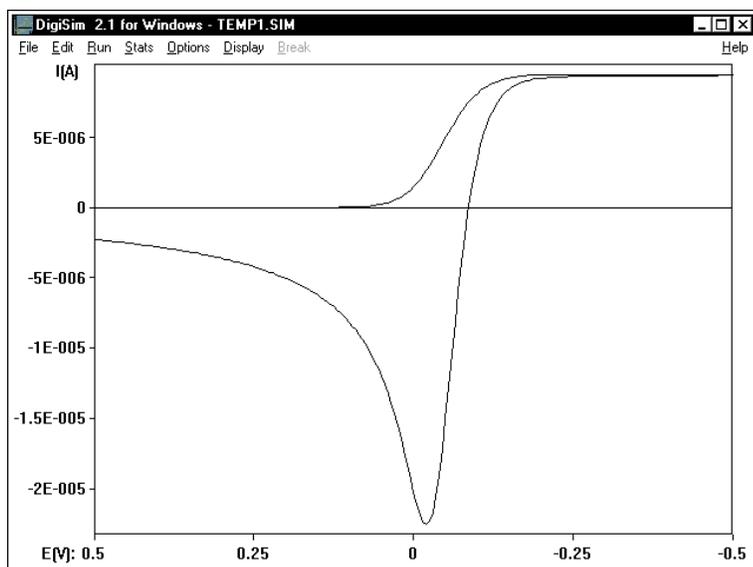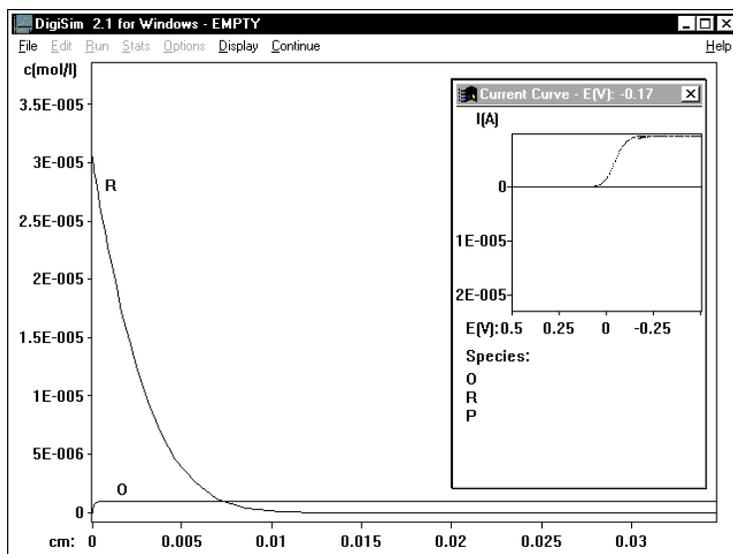
CE (1,4)

$P = O$

$O + e = R$

F1

Simulated voltammogram for O + e = R under reversible conditions.

F2

Simulated voltammogram for CE mechanism. $K_{eq}=0.001$ and $k_f/v=1V^{-1}$.

F3

CV-the Movie frame showing concentration profiles of O and R at a potential in the current plateau of the simulated voltammogram shown in F2.


This mechanism requires a system in which two species are in equilibrium, with only one species being electroactive (O). The appearance of the voltammograms will therefore depend upon the equilibrium constant for these two species, as well as k/v. **F2** shows the simulated voltammogram at $K_{eq} = 0.001$, and $k = 1\ s^{-1}$. The current response on the forward scan is indicative of steady-state behavior (i.e., it is sigmoidal rather than peak-shaped), whereas the reverse scan shows a peak, and the current is much larger. This can be rationalized as follows. On the forward scan, the concentration of O at the electrode surface is very small. However, the reduction of O perturbs the equilibrium between P and O and causes the conversion of P to O in order to restore equilibrium. Therefore, the rate of electrolysis (and hence the current) is determined by the rate of conversion of P to O (i.e., the current is kinetically controlled). The R generated by the reduction of O accumulates in the diffusion layer *(F3)* (this concentration-distance profile was generated using CV–the Movie™, part of the DigiSim program), and is available for reoxidation on the reverse scan (i.e., the current is diffusion-controlled).

As K_{eq} is increased, the current response tends toward diffusion control on both the forward and reverse scans, until a reversible voltammogram is observed at a K_{eq} value between 10 and 100 *(F4)*. The effect of varying k/v at a fixed value of K_{eq} is shown in **F5**. For small k/v, the chemical reaction has little effect, and the voltammograms show reversible behavior, with the peak current being determined by K_{eq}. As k/v increases, both the peak currents increase, but the peak current ratio is larger than 1 (for the reason described above). In the limiting case of high k/v, the voltammogram shows reversible behavior, but the peak currents are larger, and the peak potentials are shifted in a negative direction relative to the voltammogram for small k/v.
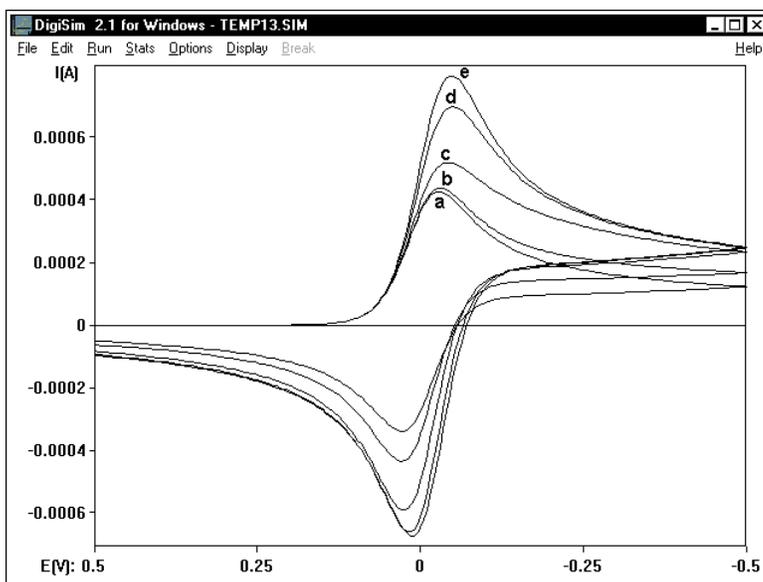
F4

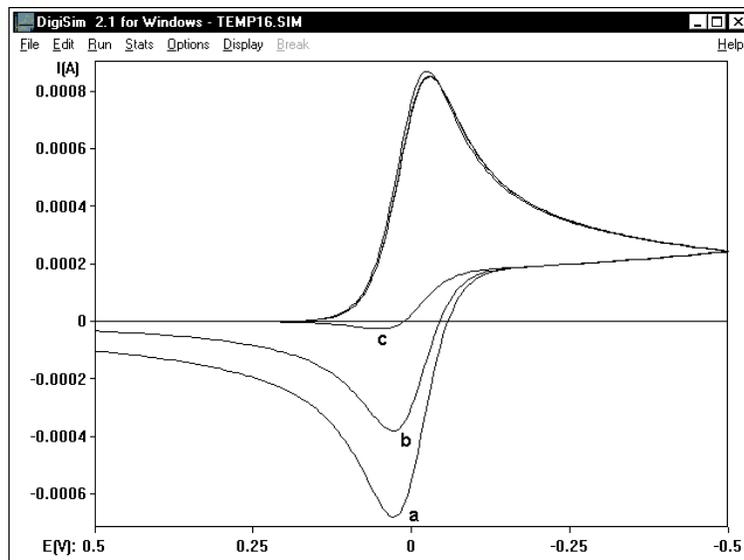*Simulated voltammograms for a CE mechanism. K_{eq}=0.001 (a), 0.01 (b), 0.1 (c), 1 (d), 10 (e), 100 (f), and k_f/v=1V^{-1}.*
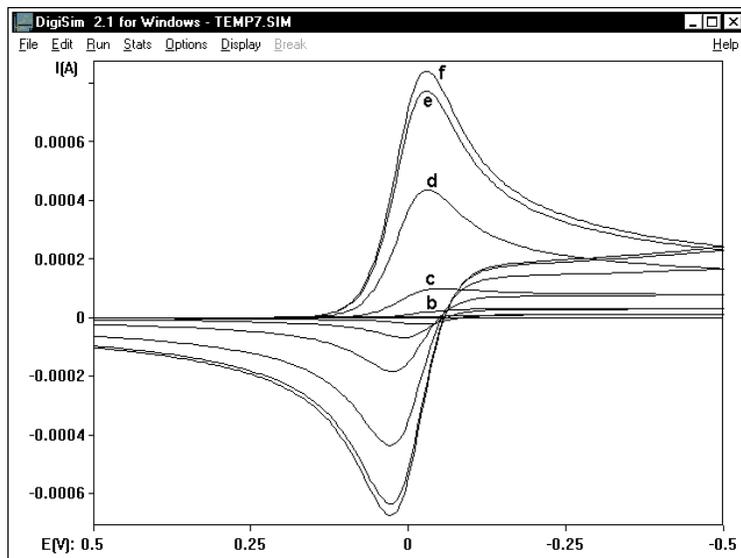
F5

Simulated voltammograms for CE mechanism. K_{eq}=0.001 and k_f/v= 0 (a), 1 (b), 10 (c), 100 (d), 1000 (e)V^{-1}.
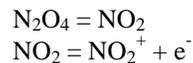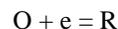

F6

Simulated voltammograms for EC mechanism. K_{eq}=10,000 and k_f/v= 0 (a), 1 (b), 10 (c)V^{-1}.

An example of a CE mechanism is the dissociation of N_2O_4 (5):

$$N_2O_4 = NO_2$$
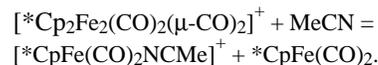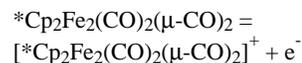$$NO_2 = NO_2^+ + e^-$$

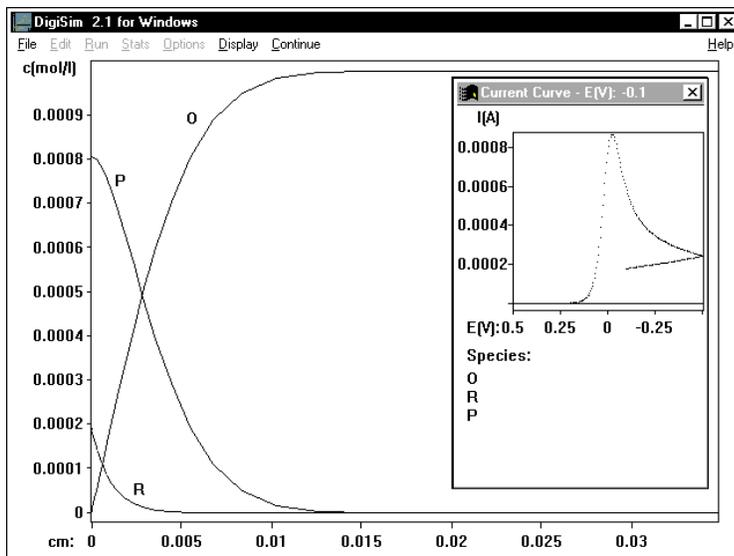**EC** (1,6)

$$O + e = R$$
$$R = P$$

The simulations for this mechanism were based on an equilibrium constant of 10^4 for the chemical reaction. At low values of k/v, the most notable characteristic of the voltammograms is the decrease in the peak current for the anodic peak with increasing k/v (**F6**). This can be related to the depletion of R in the reaction layer due to its reaction to form P (this is shown in **F7**). At sufficiently high values of k/v, there is no longer any significant anodic peak. However, increasing the value of k/v does cause further change in the voltammograms, namely a shift of the cathodic peak potentials in a positive direction (**F8**) (by about 29 mV for each decade change in k/v). As k/v is increased to higher values, the anodic peak reappears, and the limiting voltammogram for high values of k/v has the appearance of a reversible voltammogram, but it is located at potential positive of that of the voltammogram for k/v = 0 (**F9**) (the potential shifts by 59 mV with each decade increase of the equilibrium constant). The reappearance of the anodic peak shows that the reverse chemical reaction occurs at a significant rate at high values of k/v (note that the same equilibrium constant was used for all simulations in this example; therefore, as k/v increases, the rate constant for the reverse chemical reaction also increases).

One example of an EC mechanism is the oxidation of *$Cp_2Fe_2(CO)_2(\mu$-CO$)_2$, followed by the reaction of the oxidized complex with acetonitrile (7):

$$*Cp_2Fe_2(CO)_2(\mu\text{-}CO)_2 = [*Cp_2Fe_2(CO)_2(\mu\text{-}CO)_2]^+ + e^-$$

$$[*Cp_2Fe_2(CO)_2(\mu\text{-}CO)_2]^+ + MeCN = [*CpFe(CO)_2NCMe]^+ + *CpFe(CO)_2.$$

F7

CV-the Movie frame for an EC mechanism. K_{eq}=10,000 and k_f/v= 100V^{-1}.

F8

Simulated voltammograms for EC mechanism. K_{eq}=10,000 and k_f/v= 0 (a), 1000 (b), 10,000 (c), 1 x 10^5 (d), 1 x 10^6 (e)V^{-1}.

F9

Simulated voltammograms for an EC mechanism. K_{eq}=10,000 and k_f/v= 0 (a), 1 x 10^6(b), 1 x 10^{12} (c)V^{-1}.

(note that the 17 electron radical generated by the dissociation of the Fe-Fe bond undergoes further chemical reactions).

EC Catalytic (EC$_{cat}$)

$$O + e = R$$
$$R + A = O + B$$
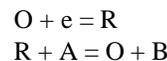
In the previous section, the effect of a first-order chemical reaction following the electron transfer reaction was discussed. In this section, the chemical reaction is again subsequent to the electron transfer reaction, but in this example the chemical reaction is second-order and involves a homogeneous electron transfer between the two reacting species (R and A) to regenerate the starting material (O).

Simulated voltammograms for the EC$_{cat}$ mechanism at different values of k/v are shown in **F10**. As k/v is increased, the current changes from diffusion-control to control by the kinetics of the catalytic reaction. At k/v = 1000, a steady-state (sigmoidal) current response is attained; this shows that the rate of removal of O by the heterogeneous electron transfer reaction is balanced by the rate of generation of O by the homogeneous electron transfer reaction.

One common EC$_{cat}$ mechanism is the oxidation/reduction of an active site of an enzyme (e.g., GOX(ox)) using a mediator (Os(polyvinylimidazole)) *(F11)*.
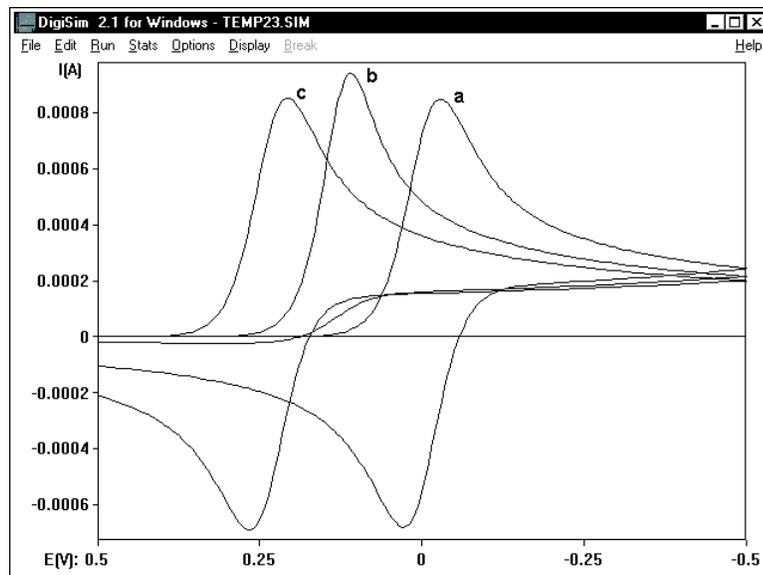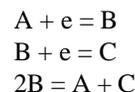
EE-Disp

$$A + e = B$$
$$B + e = C$$
$$2B = A + C$$
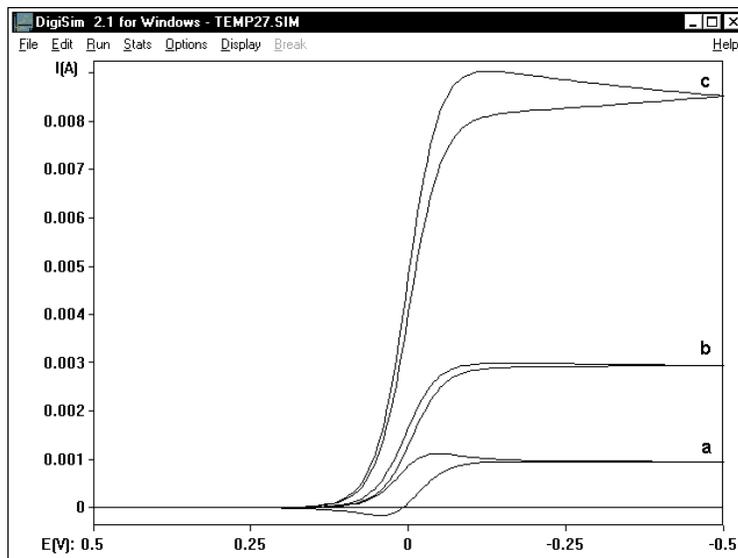
Although two-electron transfer reactions are often considered only in terms of the two one-electron transfer reactions, a disproportionation reaction (2B = A + C) should also be considered, as it can have a significant effect on the current response. One such example is shown in **F12**. In these simulations, the redox potential of the second electron transfer reaction is 100 mV positive of that of the first electron transfer
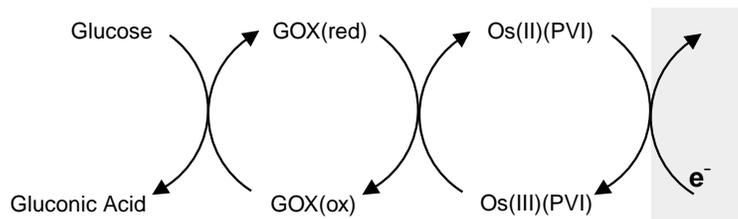
12

DigiSim 2.1 for Windows - TEMP27.SIM

Glucose → GOX(red) → Os(II)(PVI)

Gluconic Acid ← GOX(ox) ← Os(III)(PVI)

e⁻

DigiSim 2.1 for Windows - TEMP3.SIM

$2I^+ \rightleftharpoons I^{2+} + II$
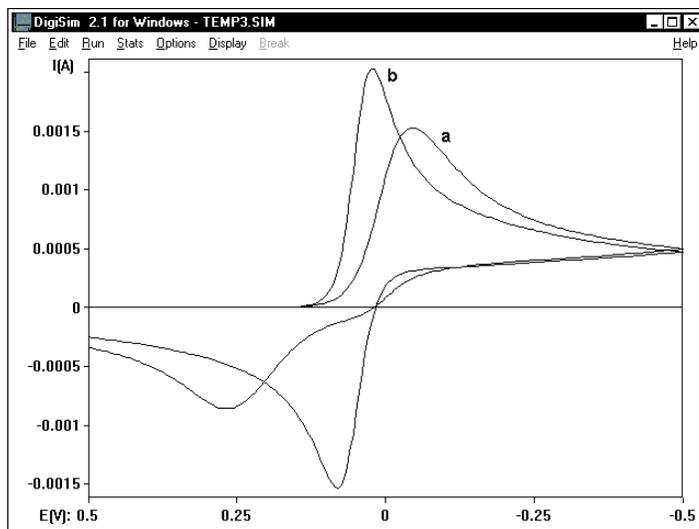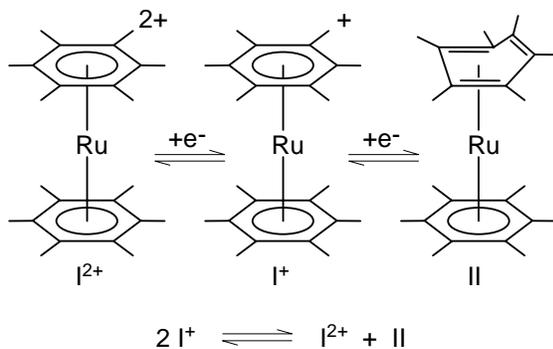
reaction; therefore, only a single two-electron transfer process is observed (8,9). The shape of the voltammogram is influenced not only by the separation of the redox potentials, but also by the kinetics of the two electron transfer reactions. In this example, the rate of the second electron transfer reaction is relatively slow (0.001 cm s⁻¹), and, in the absence of the disproportionation reaction, this has a pronounced effect on the anodic peak, with a less marked (but still significant) effect on the cathodic peak *(**F12a**)*. Incorporation of the disproportionation reaction generates the voltammogram shown in ***F12b***, in which ΔE_p and the width of both peaks have all decreased. The shape of the voltammogram in ***F12b*** approaches that expected for a reversible "two-electron" process when the two redox potentials are separated by 100 mV; that is, the slow rate for the second electron transfer reaction has little effect. This can be attributed to the fast disproportionation reaction (k = 1 x 10⁸ M⁻¹s⁻¹), which provides an alternative route for the interconversion of B and C.

One example of an EE-Disp mechanism is the two-electron reduction of [(η^6-C_6Me_6)$_2$Ru]$^{2+}$ *(**F13**)* (10).

ECE-Disp

A + e = B
B = C
C + e = D
A + D = B + C
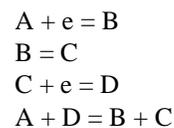
Another common "two-electron" reaction involves two one-electron transfer reactions with an intermediate chemical reaction. The current response depends upon the relative values of the redox potentials of the two electron transfer reactions and the rate of the chemical reaction. For a "two-electron" reduction, if the redox potential of the second reduction is at least 100 mV more negative than that of the first reduction, then the two processes can generally be resolved. However, if the redox potential of the second reduction is positive of that of the first reduction,

13

then a single "two-electron" reduction will be observed, as the second reduction will occur at the potential required for the first reduction. In the simulations shown in *F14*, the two redox potentials are separated by 200 mV. If the intermediate chemical reaction is not considered (*F14a*), then a reversible one-electron process is observed. However, as the value of k/v is increased, the current for the oxidation of B decreases, whereas that for the oxidation of D increases (i.e., the combination of the chemical reaction and the second reduction results in the net conversion of B to D). The cathodic peak current also increases as the net number of electrons involved in the reduction increases from 1 to 2, and the peak for the reduction of C appears on the second cathodic scan (note that the second cathodic scan is not shown in the simulations).

As indicated above, a homogeneous second-order electron transfer reaction can also be associated with an ECE mechanism. This reaction increases the rate at which A is consumed, and the rate at which C is generated. This is reflected in variations in the relative magnitude of the peak currents on the second and subsequent cathodic scans (11) (i.e., the peaks for the reduction of A and C). The equilibrium constant for this reaction is determined by the redox potentials of the two electron transfer reactions—in this example, it has a value of 0.0004. Although this value might suggest that this reaction cannot be effective, it is important to note that equilibrium cannot be realized due to the rapid conversion of B to C; that is, the chemical reaction (B = C) drives the second-order reaction. Simulations of the cyclic voltammograms of $[Rh(\mu\text{-}^tBu_2P)(CO)_2]_2$, for which the intermediate chemical reaction is an isomerization reaction (*F15*), were only possible if the homogeneous electron transfer reaction was included in the mechanism (11).
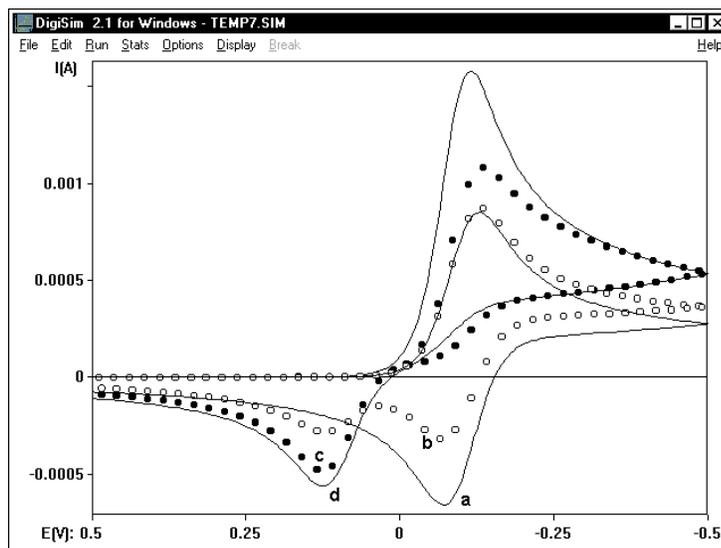
Square scheme

$$A + e = B$$
$$\| \qquad\qquad \|$$
$$D + e = C$$
$$A + C = B + D$$
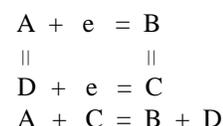
This reaction mechanism is commonly observed for electroactive molecules that can exist as more than one isomer; for example, *mer* and *fac* isomers of transition metal complexes (*F16*) (12-14). The driving force for this mechanism is the difference between the relative stability of the two isomers in the different oxidation states; that is, changing the oxidation state triggers an isomerization reaction. Since the rates of the two isomerization reactions may be very different in the two oxidation states, the current response may vary considerably with k/v. The homoge-
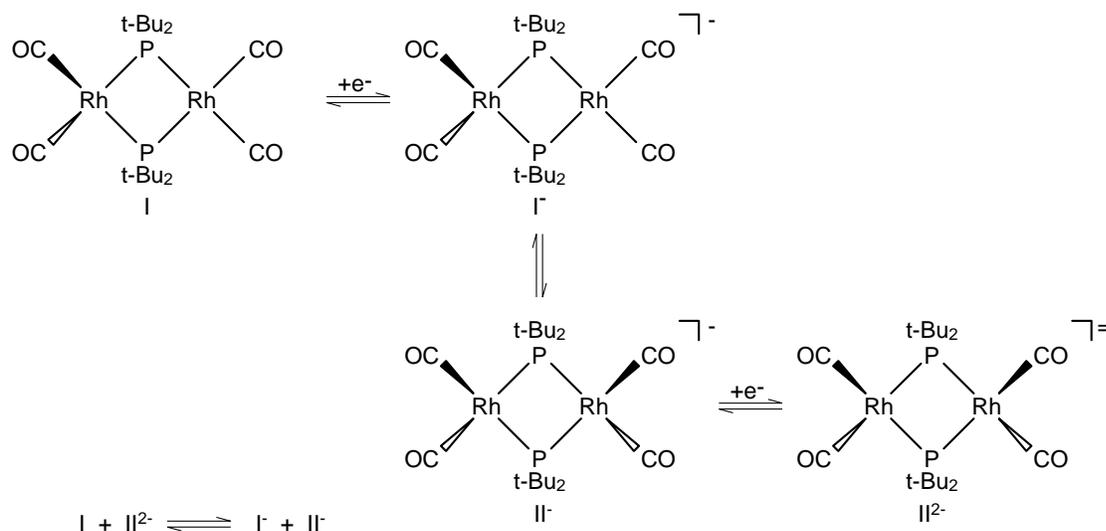
Simulated voltammograms for an ECE mechanism. $E^0_1 = -0.1V$, $E^0_2 = +0.1V$, $K_{eq} = 1 \times 10^5$, and $k_f/v = 0$ (a), 1(b), 10 (c), 100 (d) V^{-1}.
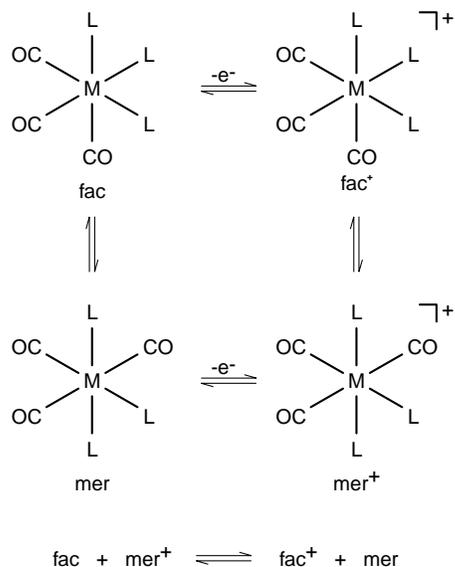

F15

Two-electron reduction of $[Rh(\mu\text{-}^tBu_2P)(CO)_2]_2$.

neous electron transfer reaction can also affect the current response.

Since there is more than one chemical reaction to be considered, all the simulations for this example were run using the same parameter set (**F17**) at different scan rates. **F18a** shows the simulation run at 10,000 V s^{-1}. Only one process is seen, which can be assigned to the A/B redox couple; that is, the scan rate is sufficiently fast that the chemical reactions have no significant effect. In contrast, at a scan rate of 0.01 V s^{-1}, the rate of the reactions that interconvert B and C (i.e., both the forward and reverse chemical reactions) are rapid relative to the scan rate. Therefore, equilibrium is maintained between B and C, and only one process is observed (**F18b**), the potential of which is intermediate between those of the A/B and C/D couples. At an intermediate frequency (100 V s^{-1}), the B/C isomerization reactions are fast enough to be significant, but not fast enough to maintain equilibrium. Therefore, both processes (A/B and C/D) can be observed (**F18c**). Detailed analysis of this behavior using CV—the Movie has been given elsewhere (13).

Although the homogeneous electron transfer reaction was not considered in the above example, it has been shown that it can have a significant effect on the relative magnitudes of the peak currents for the different isomers (13,15).

The above examples show that different mechanisms can give rise to characteristic cyclic voltammograms. It should be noted that, for most of the examples, part of the characteristic behavior involved the variation of the shape of the voltammogram with the kinetic parameter, k/ν. Therefore, variation of the scan rate (and also the temperature, if possible) should be an integral part of any mechanistic study involving cyclic voltammetry.

DigiSim is a registered trademark and CV—the Movie is a trademark of Bioanalytical Systems, Inc.

F16

Square scheme for the interconversion of geometric isomers in different oxidation states.

fac + mer$^+$ ⇌ fac$^+$ + mer

F17

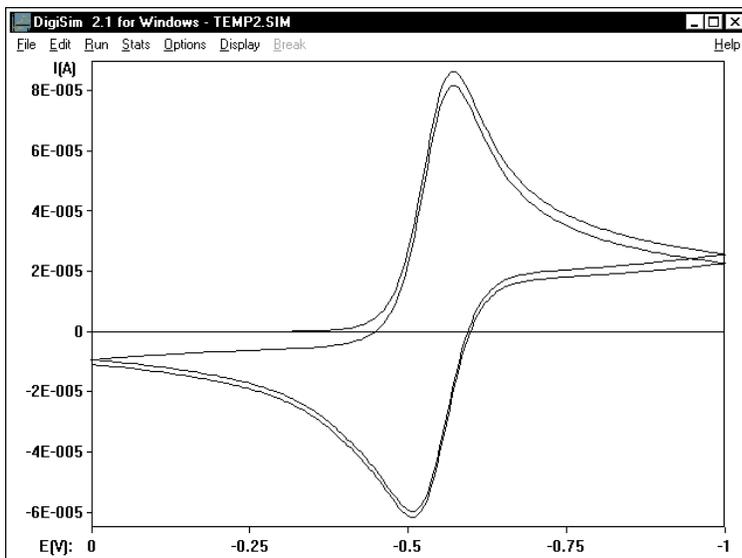*Simulation parameters for a square scheme mechanism.*

F18a

*Simulated voltammograms for square scheme mechanism using the parameters shown in **F17**. Scan rate = 10,000 V s^{-1}*
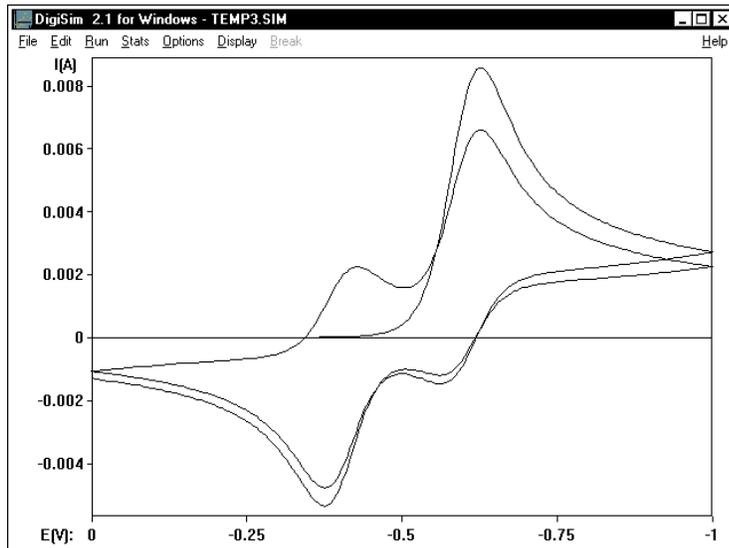
F18b

Simulated
voltammograms for
square scheme
mechanism using the
parameters shown in **F17**.
Scan rate = 0.01 V s^{-1}

F18c

Simulated
voltammograms for
square scheme
mechanism using the
parameters shown in **F17**.
Scan rate = 100 V s^{-1}

References

1. R.S. Nicholson and I. Shain, Anal. Chem. 36 (1964) 706.

2. The exact value of the peak potential separation varies with the difference between the peak potential on the forward scan and the first switching potential.

3. DigiSim is based on the principle of microscopic reversibility, so the reverse chemical reaction must always be considered. Therefore, chemical reactions are defined using an equilibrium constant and the rate of the forward reaction.

4. J.M. Saveant and E. Vianello, Electrochim. Acta 8 (1963) 905.

5. K.Y. Lee, C. Amatore and J.K. Kochi, J. Phys. Chem. 95 (1991) 1285.

6. L. Nadjo and J.M. Saveant, J. Electroanal. Chem. 48 (1973) 113.

7. J.R. Bullock, M.C. Palazzotto and K.R. Mann, Inorg. Chem. 30 (1991) 1284.

8. A.W. Bott, Curr. Separations 16 (1997) 61.

9. R.L. Myers and I. Shain, Anal. Chem. 41 (1969) 980.

10. D.T. Pierce and W.E. Geiger, J. Am. Chem. Soc. 114 (1992) 6063.

11. J.G. Gaudiello, T.C. Wright, R.A. Jones and A.J. Bard, J. Am. Chem. Soc. 107 (1985) 888.

12. W.E. Geiger, Prog. Inorg. Chem. 33 (1985) 275.

13. A.M. Bond, S.W. Feldberg, H.B. Greenhill, P.J. Mahon, R.Colton and T. Whyte, Anal. Chem. 64 (1992) 1014.

14. A.W. Bott, Curr. Separations 13 (1994) 45, 49.

15. T.C. Richards and W.E. Geiger, J. Am. Chem. Soc. 116 (1994) 2028.